Determining the wavelength and refractive index of a glass using a Michelson Interferometer

Sara Capdevila Solé

***Abstract*—This paper demonstrates an experiment aimed at investigating the wavelength and the refractive index using a Michelson interferometer provided by Imperial College London, where the setup has been constructed and thoroughly calibrated and aligned. By displacing a mirror in one of the arms, the wavelength of a red laser beam was found to be $\lambda_0 = (648 \pm 28)nm$ - 0.07 standard deviations away from the companies claimed value of $650nm$. Varying the angle of incidence of the laser beam on a microscope slide yielded a refractive index of glass $n_{gl} = 1.51 \pm 0.08$, which includes the accepted value of 1.515. This experiment has been successful, however, further measures to minimise errors and achieve a greater level of precision are proposed.**

I. Introduction

OPTICAL interferometers are widely used to extract information about waves, on a nanoscale precision. These range from applications in atomic physics, to measure the hyperfine structure, into space, where they are used in the detection of gravitational waves [1]. These devices superimpose waves, to produce interference patterns composed of fringes - interferograms [2]. A specific mode; the Michelson interferometer, presents a useful tool in measuring the wavelength of light and the refractive index of a transparent slide. This is achieved by varying the optical path difference between two beams of light; which can be adjusted by moving one of the mirrors, or by rotating the slide.

II. Experimental theory

A. A Michelson Interferometer

A Michelson interferometer works by splitting the amplitude of the light source into two. Each will travel a corresponding optical path, which will produce an interference pattern as they superimpose at recombining, according to their optical path difference (OPD). The schematic of a typical apparatus is shown in Fig. 1.

As the OPD between both arms is changed, so does the interference pattern and the corresponding fringes visible.

B. Interference

Two coherent, monochromatic beams travelling along the same path will interfere according to the principle of superposition - that is, the resulting field of the wave will be given by the vector sum of each [3].

The resulting wave will depend on the OPD between the individual waves. Maximas are produced when their OPD is an integer number of wavelengths, and Minimas when their

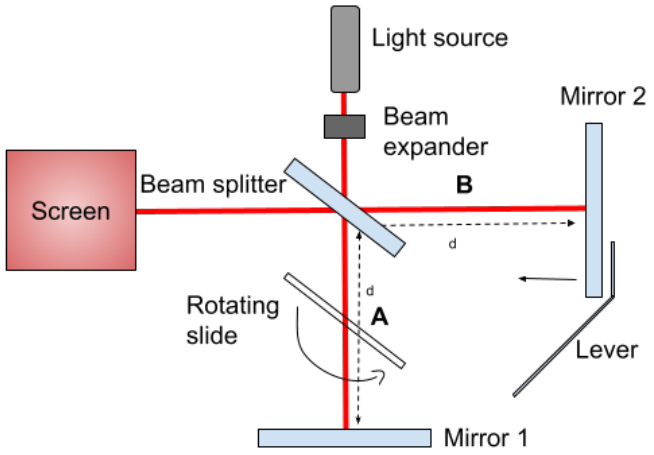

Fig. 1. **Illustration of a Michelson Interferometer:** The light source, enlarged by a beam expander (BE), hits the beam-splitter (BS); will allow 50% of light to travel through each arm of the interferometer; to mirror 1 (M1) and to a movable mirror (M2) (using the lever), later returning to the BS, forming an interference on the screen. A microscope slide (MS) is placed in arm A, such as to vary the optical path of light, by rotating it. Similarly, M2 may be moved to achieve the same result with arm B.

OPD is a half-integer number of wavelengths. As a result, Braggs law can be defined as follows [4],

$$2d \sin \phi = N\lambda \tag{1}$$

where λ is the wavelength, N is the shift in number fringes through an OPD of d, at an angle ϕ between the mirrors. The factor of 2 arises from the beam travelling through each arm twice.

The interference pattern is a series of concentric fringes. By fixing the mirrors perpendicularly (i.e. $\phi = \pi/2\ rads$). As we vary d, the central fringe can be observed to shift from dark to bright every $\lambda/4$. Counting the shift in central fringe, allows us to determine λ using;

$$\lambda = \frac{2d}{N}. \tag{2}$$

C. Refractive index

Similarly, the OPD can be varied by introducing a MS, of refractive index n and width w in one of the arms, and rotating it. Using (2), we can substitute for the OPD introduced by the MS;

$$\lambda = \frac{2(n_a d_a(\theta) + n_{gl} d_{gl}(\theta))}{N}, \tag{3}$$

where the subscript 'a' defines the refractive index and path travelled in air (n_a and d_a), and similarly for glass (n_{gl} and d_{gl}).

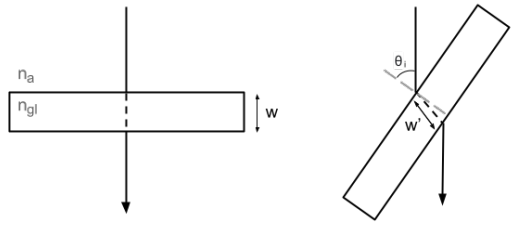

Fig. 2. **Optical path:** Introduced by the MS, by varying (θ).

Using the geometry of Fig. 2, and rearranging using Snell's law [2], we obtain[1];

$$N = \frac{2w\left(1-\cos\left(\theta_i\right)\right)\left(n_{gl}-1\right)}{n_{gl}\lambda - \lambda\left(1-\cos\left(\theta_i\right)\right)} \tag{4}$$

for an angle of incidence with the glass in the range of $(-\pi/4 < \theta_i < \pi/4)\ rads$.

D. Fringes

The interference between the waves will produce a pattern on the screen, as shown in Fig. 3. Whenever M1 and M2 are perfectly perpendicular, fringes of equal inclination will form - known as Haidinger fringe (Fig. 3 a).

However, if one is at a slight angle (ϕ), the screen will record a sinusoidal pattern (Fig. 3 b). These are equally spaced - Fizeau fringes.

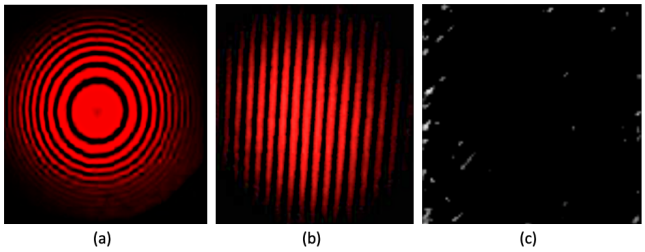

Fig. 3. **Types of fringes on the screen [2]:** a) Haidinger fringes b) Fizeau fringes c) Dark-field

When Haidinger fringes are present, the OPD is decreased. According to (1), N will also decrease. The interference pattern as a result will vanish when $d = 0$. This is known as the dark-field [3] (Fig. 3 c), and will be used as a reference point in this experiment.

III. Pre-experimental procedure

Before proceeding with the experiment, it is necessary to ensure the Michelson Interferometer is aligned and calibrated, following laser safety protocols at all times.

[1]For further information on deriving this equation please see lab book (Interferometry/refractive-index section)

A. Alignment

The setup is built as follows. The laser holder containing the laser is fixed in place. By taking out the BS and the BE initially, the adjustable screws in the components are used to ensure there is a perpendicular alignment between the laser beam and M2 (i.e. the laser beam propagates straight into the centre of M2, reflecting light perfectly into the laser). The BS is then placed at $\pi/4\ rads$ to the laser beam; which is measured using a protractor to the accuracy of a degree. The position of M1 is adjusted in the same manner as M2, using the reflected beam.

The paths A and B are made equal to $1mm$, using a ruler. This is the range in which d will be varied. This must be less than the coherence length of the light source such as to observe good interference.

The reflected beams from M1 and M2 pass through the BS again and are illuminated on the screen. Final adjustments in the screws of both mirrors are made such as to ensure these two points superimpose. When the MS is introduced into A, Fresnel reflection takes places at its surface, requiring the adjustment of the two more incoming beams, to also coincide on the screen.

The screws are fixed tightly such as to reduce the phenomena of oscillating fringes, however, these are not overdone such as to disfigure the components in the setup.

The BE is then placed, to observe the interference pattern on the screen (section II. D). The bolts on the back of M1 are adjusted until circular fringes are shown in the centre of the screen. Once this is achieved, M2 is moved using the micrometre lever to achieve the dark-field.

This position is an abstract concept and difficult to achieve, as any small air currents or vibrations will alter d (causing a drift in N).

B. Calibration

The position of M2 is adjusted (slowly) using a lever arm. The corresponding change in position of M2 can be measured using a micrometre (to an accuracy of $\pm 0.5\mu m$), and as a result, a relationship can be empirically found relating the position of M2 (P_{M2}) and change in lever position (P_L). It is made sure that the lever arm isn't touching the base of M2, such as to alter the data. This is fitted in Fig. 4.

By approximating the relationship to linear in a small region, a calibration value of $K = 0.043 \pm 0.001$ is obtained. This value will be used in the same range for the proceeding experiments.

IV. Experimental procedure

The following section describes what results have been obtained. Data in both experiments have been recorded using a slow-motion camera, to minimise random errors. Differences when repeating the experiment twice were still present. Here we've used the standard deviation in N to represent its error.

The setup is placed on top of foam to reduce the propagation of vibrations. Additional subjecting materials (e.g. a piece of paper) are also placed in air-gaps to fix their position. As a sanity check, before each experiment, the setup is touched to ensure no fringes drift.

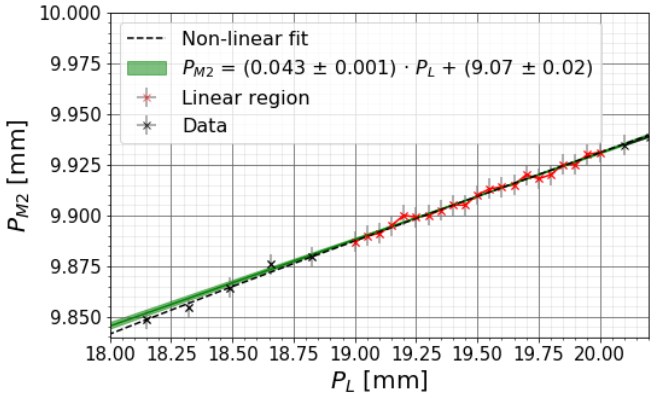

Fig. 4. **Calibration plot:** The linear calibration region are data points marked in red with their error. The linear fit and associated error (the co-variance of the data) is shown in green.

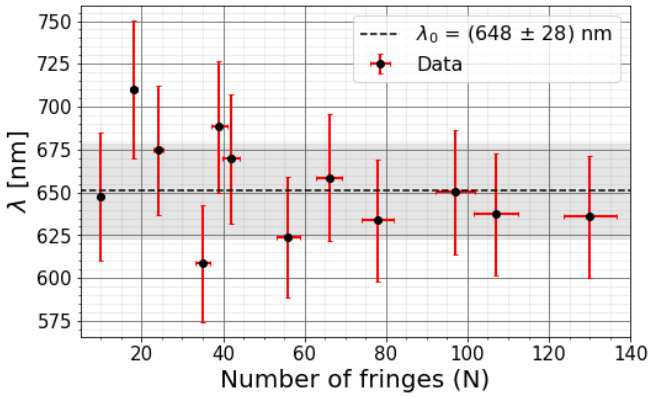

Fig. 6. **Weighted average wavelength** (λ_0) - The wavelength and its error is calculated for each N, using propagation of uncertainties from (2) . A standard deviation of λ_0 is also shown in grey.

A. *Wavelength of the laser beam*

The position of M2 is varied from the dark-field (OPD = δP_M), and N fringes appearing from the centre are counted. Fig. 5 shows the linear relationship obtained.

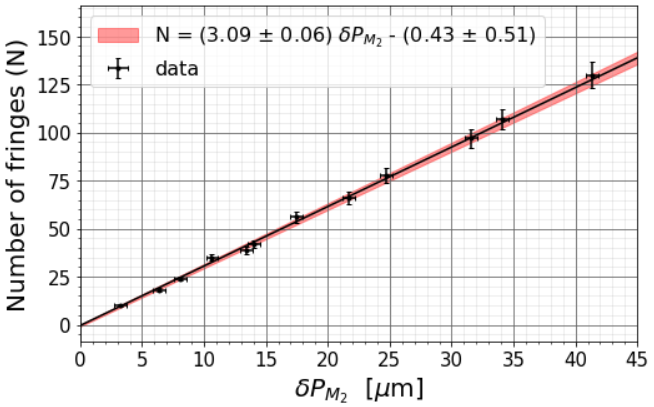

Fig. 5. **Wavelength regression plot:** Linear relationship and error between the position of M2 and the fringe variation (in red).

Using (2) and the gradient in Fig. 5, the wavelength is found; $\lambda_0 = (648 \pm 13)nm$. This uncertainty arises from the error in the fit, however, to evaluate the empirical spread in our experiment, the standard deviation of the data is calculated - relative to the weighted mean λ_0. This is shown in Fig. 6. The values for the wavelength are seen to converge to λ_0 as N increases.

The final value obtained for $\lambda_0 = (648 \pm 28)nm$, which lies 0.07 standard deviations away from the companies claimed value of $650nm$ [5], agreeing with it.

B. *Refractive index of glass*

A MS of width $w = (1.46 \pm 0.01)mm$ is rotated from a normal incidence of the beam (θ_i), and the change in N is recorded. The dark-field condition determines when $\theta_i = 0$ $rads$. This is done for both sides and an average is calculated; shown in Fig.7.

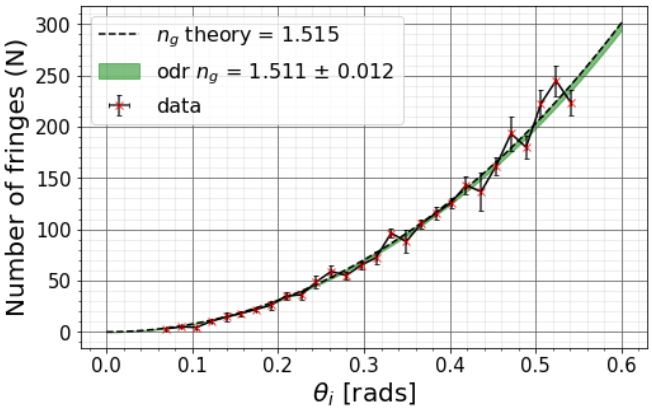

Fig. 7. **Fringe response to the rotation of MS:** An ODR fit (*Scipy* package on python) is used, and the error arises from the co-variance of the data (in green).

The value for n_{gl} is determined using an ODR fit on (4) (to account for the errors in θ_i as well as in N); $n_{gl} = 1.511 \pm 0.012$. Similarly to before, the weighted standard deviation of the data is calculated, and a final value of $n_{gl} = 1.51 \pm 0.08$ is acquired. This value lies 0.06 standard deviations away from the accepted value for Crown glass of 1.515; at a wavelength of $632.8nm$ [6], also agreeing. This experiment cannot determine the type of crown glass, due to its lack of precision.

Crown glass is the most commonly used type of MS, due to its low chromatic dispersion (high Abbe number [6]). Nonetheless, parasitic propagation is accounted for in the co-variance of the fit in Fig. 7.

V. Error Analysis

The setup was carefully aligning and adjusted to minimise errors. Dynamic errors arising from hysteresis and n_a fluctuations during the experiment have not been quantitatively evaluated, as these were assumed to be smaller and thus included in the variability (standard deviation) of the dependent variable (N). These were minimised by turning off room heating and carrying out the investigation in the most optimum accessible

environment and time (e.g. less vehicle movement during the evening). Hysteresis was considered negligible, as in-order to reduce these mechanical drifts, the direction of rotation throughout a run wasn't altered [7]. As a result, the error in the micrometre reading and rotating stage was approximated to half the smallest division on its scale ($0.5\mu m$).

At larger angles of incidence, as seen in Fig. 7, the fractional uncertainty associated with our measurements increases. This is due to the prolonged periods the experiment was carried out for, predisposing the system to more external factors. Also, the sensitivity to a small change in angle is larger as θ_i increases, as the gradient is greater.

Surface imperfections on mirrors could give rise to uneven and multiple internal reflections (e.g. not 'silvered' enough or scratches and differences in surface depth). This in principle, could give rise to non-uniform spacing between fringes; making it responsible for the large variation in N. This could also result from a non-monochromatic laser beam.

Had more data been taken for λ and n_{gl}, our standard deviations could've been smaller and our average values could've converged stronger to their theoretical counterparts.

Nonetheless, our results susceptibility to changes in other external conditions is quite large (e.g. room temperature, pressure), reinforcing the need to repeat this experiment.

Experimental errors could be minimised further by automating the movement of the stage and M2. An algorithm could be implemented and/or an oscilloscope could be used to count fringes [3]. This would remove some sources of human error. Alternatively, the possibility of coupling our setup with a Mach-Zehnder interferometer could be explored; as this would hypothetically allow us to obtain values up to the precision of 5 s.f. [8].

VI. Conclusion

A Michelson Interferometer has been aligned and calibrated to accurately obtain the wavelength of a red laser beam and the refractive index of crown glass; by varying the optical path lengths of one of the arms of the interferometer. Interferometric and error minimisation techniques have been explored, but further improvements are proposed to be able to achieve a higher level of precision.

References

[1] S. A. et al., "Atom interferometry and its applications," *physics.atom-ph, arXiv.*, 2001.10976. Jan 2020.

[2] A. C. David Colling, Andy White, "Interferometry lab script v. 4," Imperial College London, October 2020.

[3] D. Iyer, *A Michelson Interferometric Technique for Measuring Refractive Index of Sodium Zinc Tellurite Glasses*. Lehigh University, 2006. [Online]. Available: https://books.google.es/books?id=frwjnQEACAAJ

[4] K. Modjtahedzadeh, "Wavelength and refractive indices from interferometry," 2019.

[5] "Alpec spectra red laser pointer," https://www.alpec.com/product-p/4012.htm, **[online]**. Accessed: 18.03.2021.

[6] Filmetrics, "Refractive index of bk7, float glass," https://www.filmetrics.com/refractive-index-database/BK7/Float-Glass, 2021, **[online]**. Accessed: 16.03.2021.

[7] R. Szoszkiewicz, B. Bhushan, B. Huey, A. Kulik, and G. Gremaud, "Adhesion hysteresis and friction at nanometer and micrometer lengths," *Journal of Applied Physics*, vol. 99, pp. 014 310–014 310, 01 2006.

[8] M. Galli, F. Marabelli, and G. Guizzetti, "Direct measurement of refractive-index dispersion of transparent media by white-light interferometry," *Appl. Opt.*, vol. 42, no. 19, pp. 3910–3914, Jul 2003.